Chinese Chemical Letters 35 (2024) 108709

Contents lists available at ScienceDirect

Chinese Chemical Letters

journal homepage: www.elsevier.com/locate/cclet

Development and application of photocatalytic coating for roadside NO_x mitigation in Hong Kong

Xinwei Li[a], Pengge Wang[b], Shuwen Han[a], Yu Huang[b,*], Wingkei Ho[c], Steven Sai Hang Ho[d], Shun-cheng Lee[a,*], Meng Wang[a]

[a] Department of Civil and Environmental Engineering, The Hong Kong Polytechnic University, Hong Kong, China
[b] State Key Laboratory of Loess and Quaternary Geology (SKLLQG) and Key Laboratory of Aerosol Chemistry and Physics, Institute of Earth Environment, Chinese Academy of Sciences, Xi'an 710061, China
[c] Department of Science and Environmental Studies, The Education University of Hong Kong, Hong Kong, China
[d] Division of Atmospheric Sciences, Desert Research Institute, Reno, NV 89512, United States

ARTICLE INFO

Article history:
Received 24 February 2023
Revised 27 May 2023
Accepted 19 June 2023
Available online 23 June 2023

Keywords:
Photocatalysis
Coating
NO_x mitigation
Hong Kong
Roadside

ABSTRACT

A facile chemical method for the development of photocatalytic coating products was proposed based on practical application perspective for the Hong Kong roadside nitrogen oxides (NO_x) mitigation. TiO_2-based photocatalytic coating PC-C film with crystallized size of around 5–6 nm was synthesized with the peptization of H_2O_2. The PC-C coating possesses a super-hydrophilicity surface and is proven to have a NO_x degradation rate of 46.8% with an optimum pH level of 7. In addition, the PC-C coating presents a promising photocatalytic NO_x degradation compared with other commercially available coating products and P25 when applied on two building materials of poly-methyl methacrylate (PMMA) and concrete surface. A weather resistance simulation and a 180-day on-site field trial were carried out the attenuation effects of photocatalytic coating applied in outdoor exposure. Based on epidemiological estimation and field investigation, hospital admissions for respiratory diseases (HARD) and mortality cases (MC) could be reduced with the application of PC-C coating along the street canyon. This work demonstrates the feasibility of air pollution control measures for the local roadside NO_x using photocatalytic technology, offering promising health benefits with environmental remediation.

Nitrogen oxides (NO_x, *i.e.*, NO + NO_2), as notorious atmospheric pollutants, not only promote the formation of ozone and secondary aerosols [1,2], but also exhibit adverse health effects on human with increasing respiratory deaths and lung cancer deaths [3–5]. As a densely populated urban metropolis, traffic-related emissions contributed to the majority of Hong Kong's NO_x pollution [6,7]. To improve air quality, the Hong Kong Environmental Protection Department (HKEPD) has implemented a series of emission control measures successfully contributing to the steady decline in air pollution levels in recent years [7–9]. However, challenges still exist, that is, the roadside NO_2 level still exceeds the Hong Kong Air Quality Objectives (AQO) and World Health Organization (WHO) global Air Quality Guidelines (AQG) [10,11]. Thus, innovative air pollution control technologies should be implemented at the same time to supplement the current emission control technologies.

Passive air pollution control technologies represented by photocatalytic coatings have been increasingly considered the solutions to mitigate air pollution without requiring enforcement, significant capital investments or changes in human behavior [12–16]. Photocatalytic technology, which is excited by light irradiation involving reactive radicals' oxidation process, is an ecologically and economically sustainable measure for direct air pollution control in outdoor environments [17–20]. Up to date, photocatalytic coatings have been applied to several urban microenvironments, walls and tunnels in cities all over the world, including Italy [21,22], Germany [23], the Netherlands [24], Belgium [25], Poland [26], Span [27], China [28–30], *etc.* as listed in Table S1 (Supporting information). The accepted products for the photocatalytic conversion of NO_x are NO_2^- and NO_3^-, which are harmless in small quantities and would be washed away by water droplets [31,32]. Generally, photocatalysts developed in the laboratory are in powder form and are inappropriate for real-world applications [33]. However, the limitations can be overcome by coating them on the surfaces of various substrates to immobilize those powders as films. With the consideration of the practical application, the coating products

* Corresponding authors.
E-mail addresses: huangyu@ieecas.cn (Y. Huang), shun-cheng.lee@polyu.edu.hk (S.-c. Lee).

https://doi.org/10.1016/j.cclet.2023.108709
1001-8417/

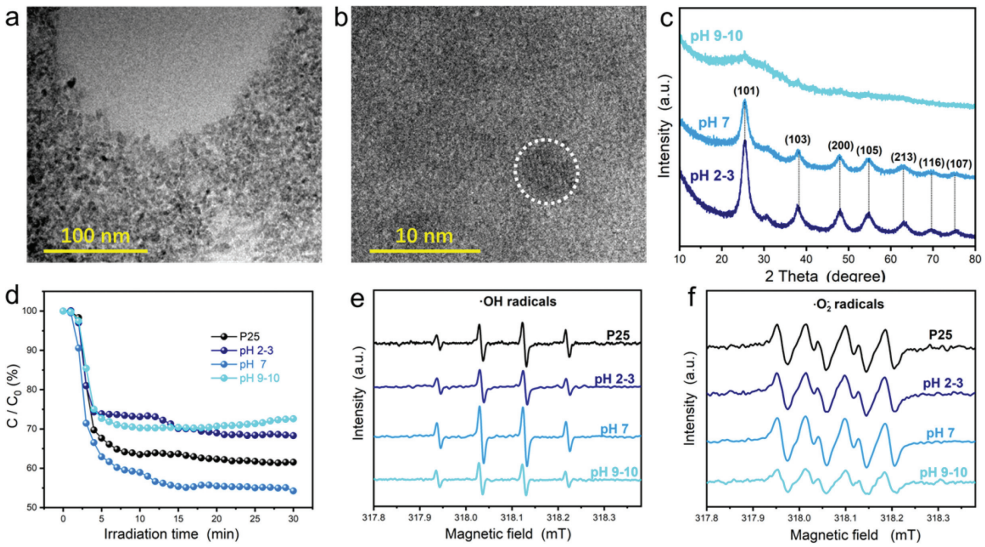

Fig. 1. TEM (a, b) of PC-C films (pH 7). XRD patterns of PC-C coating films (c) and photocatalytic activity of NO removal of PC-C coating films at different pH levels and P25 under simulated solar light (d). DMPO ESR spectra samples under simulated solar light irradiation in aqueous dispersion for DMPO-$^{\bullet}OH$ (e) and in methanol dispersion for DMPO-$^{\bullet}O_2^-$ (f).

should initially possess exceptional photocatalytic performance in NO_x degradation and provide predictable health benefits. Then, the coating films generated by facile preparation methods could be adhered to different substrates without altering or affecting any existing settings. Moreover, the physicochemical properties of coating products are expected to be stable when exposed to actual roadside environments. Therefore, the development and application of photocatalytic coating for urban roadside NO_x reduction is desirable but remains challenging.

Herein, a facile method for developing photocatalytic coating products was proposed. Two types of representative construction materials as the coating substrates were investigated, considering the wide acceptance of different substrates. An artificial weather resistance test and an on-site field trial were conducted to investigate the attenuation of the photocatalytic coating. In view of the practical outcomes, the health effects were estimated and evaluated based on epidemiological statistics.

The nanosized particles are uniformly distributed in the PC-C coating film by transmission electron microscopy (TEM), as shown in Fig. 1a, and crystallized nanoparticles around 5–6 nm in size are observed (Fig. 1b), different from the TiO_2 film synthesized through traditional sol-gel methods in bulk state or nanosized greater than 50 nm [34]. The pH level of the PC-C film without adjustment is acidic due to the mild acidity H_2O_2. Considering the acidity/alkalinity of the photocatalytic film might affect its characteristics, the catalytic performance could be also altered to some extent [35]. As shown in Fig. S5 (Supporting information), the PC-C film becomes a clear yellowish solution with desired dispersibility when the pH value is equal to or above 7. The TiO_2 film would be positively charged if the pH value is lower than the isoelectric point of 4.5–6.8 [36], which could impede the formation of TiO_2 sol and then resulting in the formation of a non-transparent colloidal solution. The crystal structures of PC-C coatings films at acid, neutral and alkaline states are displayed in Fig. 1c. The TiO_2 anatase phase (PDF #1–526) of the PC-C coating films is well-crystallized when in the acidic (pH 2–3) and neutral (pH 7) medium. When the pH level was further increases, the alkaline material would break the TiO_2 crystal structure and lead to amorphous states. The X-ray photoelectron spectroscopy (XPS) analysis presented in Fig. S6a (Supporting information) revealed the presence of Ti, O, and C in the PC-C coating films synthesized in neutral medium. The Ti 2p high-resolution spectrum (Fig. S6c in Supporting information) showed two peaks at 464.1 eV and 458.4 eV, which can be attributed to Ti^{4+} in TiO_2. Additionally, the O 1s spectrum (Fig. S6d in Supporting information) exhibited two distinct peaks at 532.2 eV and 529.7 eV, corresponding to surface OH and Ti-O, respectively [37].

Optical response comparison of TiO_2 (anatase) and PC-C coating films was investigated by UV–vis DRS in Fig. S7 (Supporting information). The adsorption edge of pristine TiO_2 is about 380 nm. However, the PC-C coating films is ranged from 440 nm to 480 nm. The obvious redshift of PC-C coatings was considered as the peptization of H_2O_2, which modifies the crystallized size of TiO_2 to around 5–6 nm, affecting the light adsorption ability of PC-C coating films. Photocatalytic activity of the PC-C films with different pH levels were conducted by the degradation of NO under simulated solar light irradiation in the laboratory. Material P25 Evonik (formerly Degussa) with the same content was used as a reference. As shown in Fig. 1d, the PC-C film at pH 7 showed the highest NO removal ratio (C/C_0%) that reached to approximately 46.8%, which is higher than that of P25 tested at the same conditions with NO removal rate at 38.8%. The photocatalytic activities of PC-C coating in acidic and alkaline conditions are 31.2% and 27.3%, respectively. The photocatalytic activity of the PC-C film at acid states could be affected by the incomplete sol-gel procedures, whereas the more evident decrease in the alkaline environments is due to the deterioration of the TiO_2 crystallinity. It was reported that amorphous TiO_2 would reduce the photocatalytic activity because of the facilitated recombination of the photo-formed electrons and holes [38]. Reactive oxygen species (ROS) of are detected in ESR when DMPO were selected as the trapping agent. As shown in Figs. 1e and f, the characteristic signals of both DMPO-$^{\bullet}O_2^-$ and DMPO-$^{\bullet}OH$ could be observed in the test samples. Notably, enhanced signals were observed in PC-C film at pH 7, indicating more ROS were generated under light irradiation for the following reactions [39].

In practical application, the hydrophilic surfaces could induce spread over of water droplets, where the deposited dusts and dirt are easily washed away to reach the self-cleaning effects [30]. In this study the self-cleaning capacities of the PC-C coating films were evaluated by the contact angle (CA) that was measured after Xe lamp irradiation for 3 min. As shown inn Figs. 2a-c, the CA values of the PC-C coating films at acid, neutral and alkaline conditions are 57.1°, <2.0°, and 28.8°, respectively. The PC-C films at the neutral state possessed the super hydrophilicity properties, in-

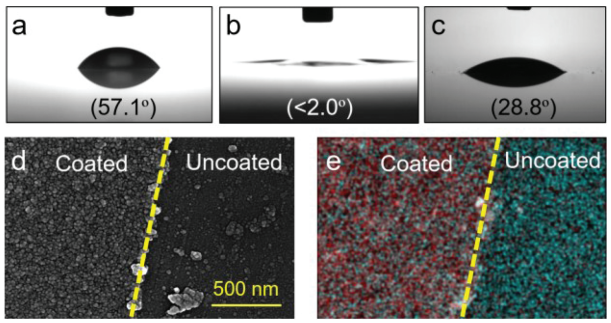

Fig. 2. CA values of PC-C films synthesized with different pH levels: pH 2–3 (a), pH 7 (b) and pH 9–10 (c). SEM image (d) and mapping analysis (e) of the high-pressure spraying coated and uncoated PC-C film on substrates, elements distribution, Ti: red, O: cyan.

dicating the most optimal self-cleaning properties. From scanning electron microscope (SEM) in Fig. 2d, the side of the coated substrate is covered with heterogeneous nanosized particles. The mapping analysis in Fig. 2e further demonstrate the even distribution of Ti and O, representing that substrates could be uniformly dispersed by high-pressure spraying.

Two types of representative construction materials were selected as the coating substrates for NO_x degradation. The first type was PMMA, which is a transparent thermoplastic, as a lightweight and shatter-resistant alternative to glass; the second type was concrete, which is a basic material for urban architecture. The two other commercial photocatalytic coating products labelled as PC-A and PC-B, as well as P25, labelled as PC-D, were also applied for comparisons. Detailed information on the coating products is shown in Table S2 (Supporting information), and the as-prepared specimens are shown in Fig. S8 (Supporting information).

The photocatalytic degradation performances of coated specimens are shown in Figs. 3a and b, respectively. PC-C-PMMA and PC-D-PMMA presented degradation ratios of photocatalytic NOx removal at 5.6% and 3.8%, respectively. The corresponding NO_2 yield ratio of PC-C-PMMA was 0.5%, which was lower than 1.4% of the PC-D-PMMA. In the concrete specimen, the NO_x removal ratios followed an order of PC-C-Concrete (28.2%) > PC-D-Concrete (26.9%) > PC-A-Concrete (18.9%) > PC-B-Concrete (2.5%) ≈ blank-Concrete (2.7%). It is worth noting that the NO_2 yield from the PC-C-Concrete is lower than that of the PC-D-Concrete specimen. In addition, the PCC-Concrete specimen demonstrates a degradation rate of approximately 17% when NO_2 is used as the initial gas (Fig. S9 in Supporting information), suggesting that the PC-C coating film has a direct effect on the degradation of NO_2. This finding implies that the installation of photocatalytic coating would not have any adverse impacts on air quality. Figs. S10a and b (Supporting information) show five-time consecutive tests of photocatalytic degradation of NO_x over PC-C-PMMA and PC-C-Concrete specimens, respectively. The two specimens present insignificant decay in photocatalytic activities, suggesting the relative stability of the PC-C over the two substrates. To illustrate the reaction mechanism of photocatalytic conversion of NO_x, the simplified photocatalytic conversion mechanism over PC-C coating is presented in Table 1.

From a practical perspective, the specific NO_x removal rate ($r(NO_x)$) on substrates is an important criterion in evaluation [40,41]. Fig. 3c clearly shows that PC-C coatings have the highest specific NO_x removal rate on PMMA and concrete surfaces with value of 1.01 and 4.84 mg m^{-2} h^{-2}, respectively. The differences in the photocatalytic activities of the two substrates are mainly due to the physical properties of the surfaces. Restricted to the adhesive ability between the photocatalytic coating products and substrate materials, there is approximately 4 mg the coating products per PMMA test specimen, with the coating content per unit area of around 0.8 mg/cm^2. However, the coating content over the concrete specimen was approximately 4.0 mg/cm^2, which had more than 300 mg coating products in total. In addition, dissimilar to relatively inert PMMA, the cement-based material is chemically linked with the photocatalytic coating, which renders better activity and stability [42].

Table 1
Photocatalytic reaction steps of NO_x over PC-C coating.

Reaction steps	Related reactions
Light excitation	PC-C coating+ $h\nu \rightarrow h^+ + e^-$
Adsorption	H_2O_{gas}, $O_{2gas} \rightarrow H_2O_{ads}$, O_{2ads}
	NO_{gas}, $NO_{2gas} \rightarrow NO_{ads}$, NO_{2ads}
Radicals' generation	$H_2O_{ads} + h^+ \rightarrow {}^{\cdot}OH + H^+$
	$O_{2ads} + e^- \rightarrow {}^{\cdot}O_2^-$
NO_x degradation	$NO_{gas}/NO_{2ads} + {}^{\cdot}OH \rightarrow HNO_2 + HNO_3$
	$NO_{gas}/NO_{2ads} + {}^{\cdot}O_2^- \rightarrow 2NO_2^- + NO_3^-$

It should be noted that NO_x^- (NO_3^- and NO_2^-) is recognised as the final products of NO_x photocatalytic oxidation [43]. The NO_x-to-NO_x^- content of the specific coating was determined by the detection of the washed residuals of the tested specimens (Fig. 3d). Even though, the NO_x degradation rates of PC-A-PMMA and PC-B-PMMA specimens are relatively low, there are 0.71 and 1.18 ug of NO_x^- were detected per milligrams of coating contents, respectively, indicating that these coating products also have NO_x degradation effects to some extent. In addition, the PC-C coating products have the highest NO_x-to-NO_x^- of 3.93 and 4.84 μg/mg on the PMMA and concrete specimen, respectively. The results are constant with that of the degradation activity test, where concrete specimens showed more NO_x^- accumulations than the PMMA specimens.

Coating products will inevitably experience the attenuation effects of nature environments when applied outdoors. The artificial accelerated aging test was conducted to explore the weather resistance, as shown in Fig. S11 (Supporting information). The comprehensive acceleration factor $AF_{T/H/UV}$ was calculated to be 103.8 considering the combined meteorological parameters of temperature, humidity, and ultraviolet radiation in Table S3 (Supporting information). This finding indicates that the as-provided seven-hour aging procedure simulated approximately 100 times, *i.e.*, 30-day of outdoor aging conditions in Hong Kong [44]. The accumulated degradation amounts of NO_x on the coated PMMA and concrete specimens that underwent artificial aging are presented in Figs. S12a, b and Table S4 (Supporting information). The 30-minute NO_x degradation amounts of PC-C coating on PMMA specimen decreased from 2.51 μg to 1.25 μg (50.2%), and that on concrete specimen reduced from 17.28 μg to 14.94 μg (13.5%), respectively. Similarly, a 71.3% NO_x degradation is observed with PC-D on the PMMA, whereas only 28.5% with PC-D-Concrete. In comparison, the coating products were proven to be more stable when applied on concrete surfaces. This could be explained as the rough and porous concrete surfaces that a provide a strong binding between the coating products and the concrete surfaces [45].

The field trial involving the PC-C specimens that experience different periods of field trial would be collected back to the laboratory for NO_x degradation activity tests. The field study would directly examine the attenuation of the coated specimens exposed in the actual environments. The field trial underwent 180 days (from 25th Oct. 2021 to 23rd Apr. 2022), and the collection time are illustrated in Tables S5 and S6 (Supporting information). Two parallel scenarios were designed in the field trials considering the role of rainfalls in outdoor environment in Fig. S13 (Supporting information). The specimen placed with a transparent cover is denoted as

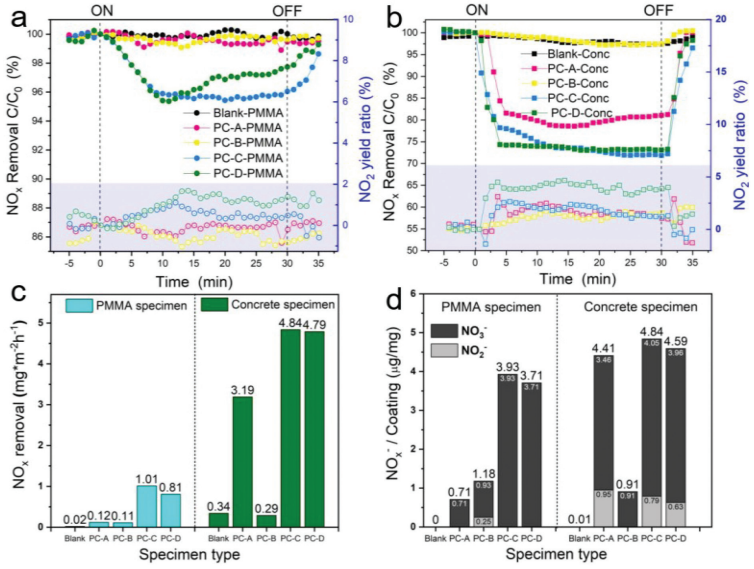

Fig. 3. Photocatalytic activity of NO_x removal of the coated PMMA (a) and concrete (b) specimen under simulated solar light (NO as the initial gas). Specific NO_x removal rate of coated specimen (c). NO_x-to-NO_2^- ratio and NO_x-to-NO_3^- ratio of the coated specimen (d).

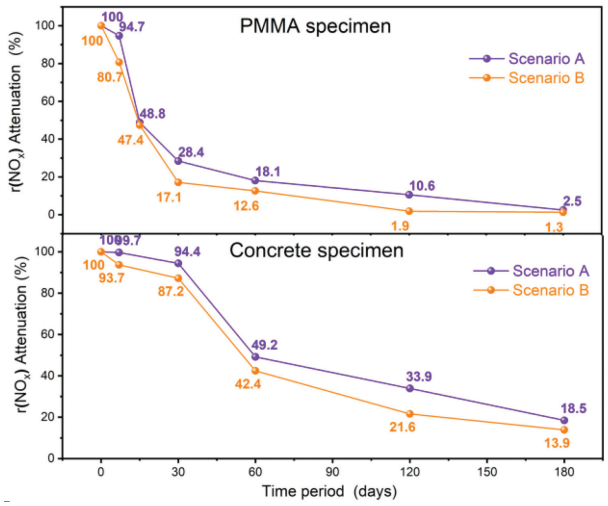

Fig. 4. Attenuation rate of $r(NO_x)$ in PC-C-PMMA and PC-C-Concrete specimen over a 180-day exposure time.

scenario A, and without a transparent cover is scenario B. The field trial did not suspend during the entire period.

Fig. 4 shows the attenuation rates of $r(NO_x)$ of the PC-C-PMMA specimen over exposure time. In scenario A with transparent shelter, the $r(NO_x)$ of the PC-C-PMMA has a decline of 48.8% from the original level after 15-day exposure, and a further drop of 18.1% after exposing for 60 days. Similarly, the declining trend of $r(NO_x)$ of the specimens in scenario B attenuated rapidly to 47.4% of the beginning level in the first 15 days and continues to decrease in the following days. The $r(NO_x)$ of the PC-C-PMMA specimens in both scenarios are almost zero, indicating no photocatalytic effects after the 180-day exposure. Eventually, the downtrend in scenario B was more distinct than that in scenario A. Fig. 4 presents the variations of $r(NO_x)$ of the PC-C-Concrete specimens in the 180-day field trials of the two scenarios. In scenario A, the $r(NO_x)$ only decayed to 94.4% after 30-day outdoor exposure, and then decreased noticeably (approximately by half) to 49.2%, experiencing 60 days of roadside environment. Only 18.5% of $r(NO_x)$ is left after completing the entire 180-day field trial. As the same observation as the

Table 2
Somatic parameters and estimated HR of NO_2 for infants, children (8–10 years old), male adults and female adults.

Age group	BR (m^3/d)	BW (kg)	DR (μg/kg)	HR
Infants	0.8	3.0	17.3	11.5
Children (8–10 years old)	10	30.0	21.6	14.4
Adults (Male)	20	74.4	17.5	11.6
Adults (Female)	20	61.1	21.2	14.1

Note: BR, breathing rate; BW, body weight; DR, dose rate.

PC-C-PMMA, the downtrend in $r(NO_x)$ of the PC-C-Concrete specimens is more evident in scenario B than A. It remained 93.7% of the initial level after the 7-day trial, and then dropped to 87.2% when the outdoor exposure time was prolonged to 30 days. The $r(NO_x)$ finally showed 13.9% of the original level after the entire 180-day trials. The detailed values of the degradation results are given in Tables S7 and S8 (Supporting information). The more intense connection between PC-C coating and concrete surface was further verified in the field trial. It is noticed that all the test specimens placed in scenario A (with a transparent cover) presented higher NO_x degradation ability than the test specimens placed in scenario B (without a transparent cover) with the same exposure time, implying that the PC-C coating possesses a relatively stable NO_x degradation when away from rainfall. Although the dirt on the surface of the specimen could be splashed in scenario B, it could inevitably affect the lifetime of the coating due to the natural attenuation by rainwater.

A pre-monitoring of air quality was performed from October 3rd-31st, 2021 at the same location to act as a reference for the NO_x concentration level. Ambient NO_x (NO, NO_2) concentrations were measured continuously using an online NO_x analyzer (200E - Teledyne API), as shown in Fig. S14 (Supporting information). The hourly averaged NO_2 concentration in the sampling month was 64.72 μg/m^3, which is much higher than AQGs with WHO and AQO with HKEPD. Furthermore, the health risk (HR) of NO_2 for different ages and gender groups based on the data collected are shown in Table 2. The results imply that children (8–10 years old) and female adults have the relatively higher HR levels of 21.6 and 21.3, respectively. Meanwhile, male adults and infants possessed relatively lower HR of 17.5 and 17.3, respectively. In comparison

with that in other studies, our average HR value obtained outside the tunnel is much higher than that in universities, tourist sites, residential areas and even factories in urban cities of China and South Korea [46,47]. It should be noted that the HR level is positively related to NO_2 concentrations, indicating the intense adverse health outcomes for roadside residents, especially for children and women. Even though, several emission control measures have been established by the Hong Kong SAR Governments, leading to a decrease in the NO_2 concentration in recent years [48,49]. The potential health hazard to roadside residents cannot be completely neglected.

The Air Quality Health Impact Assessment (AirQ+ 2.1) software based on concentration–response functions established by epidemiological studies was adopted to quantify the short-term health benefits of applying photocatalytic coating technologies at the roadside environment [50]. The model was established as a 5-km^2 street canyon, and the maximum 1-hour NO_2 of hospital admissions for respiratory diseases (HARD) and expected annual number of mortality cases (MC) based on the related attributable proportion (AP) were estimated and shown in Table S9 (Supporting information). Specifically, the average hourly NO_2 concentrations during the morning peak (07:00–10:00 LST) and evening peak (17:00–20:00 LST) on working days were 181.3 and 138.8 μg/m^3, respectively, in October 2021. With the application of the photocatalytic coating technology, it is expected to diminish the roadside NO_2 concentration to 171.1 and 130.2 μg/m^3 in the morning peak, and 131.0 and 99.6 μg/m^3 in the evening peak, with PC-C film on PMMA and concrete surface, respectively. Besides, the AP due to the exposure on the roadside NO_2 during the morning peak time was 2.5% (95%, CI:0, 6.3%) and the MC is 4.5% (95%, CI: 2.7%, 6.3%). In the evening peak time, the AP and MC are 1.9% and 3.4%, respectively. Potential health benefits of PC-C coatings applied on both PMMA and Concrete in roadside environments are expected. For example, approximately 5% and 30% reductions of HARD are found with the PC-C film on PMMA and concrete surfaces, respectively, in the morning peak hours. Therefore, the application of the PC-C coating on construction materials would effectively reduce the health expense in the roadside environment.

In summary, a facile method for the development of TiO_2-based PC-C photocatalytic coating film was prepared in this work. The nanosized PC-C coating is proven to possess a super-hydrophilicity surface and ideal NO_x degradation activity at neutral state. Both the artificial weather resistance test and on-site investigation imply that the concrete surface provides a strong bonding interaction with the coating, which is beneficial to extend the coating lifetime. Besides, the model estimates that the applications of the PC-C coating could reduce health hazards and expenses for roadside residents, especially during peak hours. This work provides a new reference for the development and practical application of photocatalytic coating for air pollution control. Even though the scale of this field trial is limited, the application of the photocatalytic coating in terms of roadside NO_x mitigation is worthwhile. A more detailed analysis regarding cost-benefits, traffic volume, and on-site monitoring in a larger scale is recommended in future studies.

Declaration of competing interest

The authors declare that they have no known competing financial interests or personal relationships that could have appeared to influence the work reported in this paper.

Acknowledgments

This work was supported by the collaborative research project from Ove Arup & Partners Hong Kong Limited (No. P0038294), Theme-based Research Schemes (Nos. T31-603/21-N and T24-504/17-N) of Research Grants Council, Hong Kong. This research is also supported by the General Research Fund, Research Grants Council of Hong Kong Government (No. 18300920) and Dean's Research Fund (No. 04738), FLASS, EdUHK. The authors are grateful to supports from the Highway Department of Hong Kong, SAR for the field study part of this work.

Supplementary materials

Supplementary material associated with this article can be found, in the online version, at doi:10.1016/j.cclet.2023.108709.

References

[1] J.H. Seinfeld, S. Pandis, Atmos. Chem. Phys. 1326 (1998) 33–38.
[2] T. Boningari, P.G. Smirniotis, Curr. Opin. in Chem. Eng. 13 (2016) 133–141.
[3] X. Lu, T. Yao, Y. Li, J. Fung, A. Lau, Environ. Pollut. 212 (2016) 135–146.
[4] A. Chauhan, H.M. Inskip, C.H. Linaker, et al., The Lancet 361 (2003) 1939–1944.
[5] M. Jerrett, R.T. Burnett, B.S. Beckerman, et al., Am. J. Respir. Crit. Care Med. 188 (2013) 593–599.
[6] P. Brimblecombe, Environ. Monit. Assess. 192 (2020) 295.
[7] HKEPD, (2021). https://www.aqhi.gov.hk/api_history/english/report/files/AQR2020e_final.pdf.
[8] Y. Huang, Z.H. Ling, S.C. Lee, et al., Atmos. Environ. 122 (2015) 809–818.
[9] L. Cui, X.L. Wang, K.F. Ho, et al., Atmos. Environ. 177 (2018) 64–74.
[10] HKEPD, (2021) https://www.epd.gov.hk/epd/sites/default/files/epd/english/environmentinhk/air/air_quality_objectives/files/Hong_kong_AQO.pdf.
[11] WHO, (2021). https://www.who.int/publications/i/item/9789240034228
[12] D. Voordeckers, T. Lauriks, S. Denys, et al., Landscape Urban Plan 207 (2021) 103980.
[13] A. Basso, A.P. Battisti, R. Moreira, H... José, Environ. Technol. 41 (2020) 1568–1579.
[14] T. Maggos, J. Bartzis, M. Liakou, C. Gobin, J. Hazard. Mater. 146 (2007) 668–673.
[15] M. Gallus, V. Akylas, F. Barmpas, et al., Build Environ. 84 (2015) 125–133.
[16] M. Cai, Y. Liu, C. Wang, et al., Sep. Purif. 304 (2023) 122401–122402.
[17] Y. Nosaka, A. Nosaka, Chem. Rev. 117 (2017) 11302–11336.
[18] C. Wang, R. Yan, M. Cai, Y. Liu, S. Li, Appl. Surf. Sci. 610 (2023) 155346–155356.
[19] S. Li, M. Cai, Y. Liu, et al., Chinese J. Catal. 43 (2022) 2652–2664.
[20] S. Li, C. Wang, Y. Liu, et al., Chem. Eng. J. 455 (2023) 140943.
[21] G. Guerrini, E. Peccati, International RILEM Symposium on Photocatalysis, Environment and Construction Materials Proceedings, Florence/Italy, 2007, pp. 179–186.
[22] M. Lettieri, D. Colangiuli, M. Masieri, A. Calia, Build. Environ. 147 (2019) 506–516.
[23] S. Jacobi, Modellversuch Fulda 12 (2012) 59–66.
[24] M. Ballari, H. Brouwers, J. Hazard. Mater. 254 (2013) 406–414.
[25] N. Bengtsson, M. Castellote, Mater. de Construccion. 64 (2014) 1–17.
[26] H. Witkowski, W. Jackiewiczrek, K. Chilmon, et al., J. Appl. Sci. 9 (2019) 1735–1744.
[27] J. Cordero, R. Hingorani, E. Jiménez-Relinque, et al., Sci. Total Environ. 766 (2021) 144393–144402.
[28] M. Chen, Y. Liu, J. Hazard. Mater. 174 (2010) 375–379.
[29] M. Chen, J. Chu, J. Clean. Prod. 19 (2011) 1266–1272.
[30] Y. Huang, J. Zhang, Z. Wang, et al., Sol. RRL 4 (2020) 2000170.
[31] J. Chen, C. Poon, Build. Environ. 44 (2009) 1899–1906.
[32] L. Yang, A. Hakki, F. Wang, D.E. Macphee, Appl. Catal. B Environ. 222 (2018) 200–208.
[33] R. Zouzelka, J. Rathousky, Appl. Catal. B: Environ. 217 (2017) 466–476.
[34] S.Y. Choi, M. Mamak, N. Coombs, N. Chopra, G.A. Ozin, Adv. Funct. Mater. 14 (2004) 335–344.
[35] L. Chen, J. Tian, H. Qiu, et al., Ceram. Int. 35 (2009) 3275–3280.
[36] N. Sasirekha, B. Rajesh, Y. Chen, Thin Solid Films 518 (2009) 43–48.
[37] Y. Chen, W. Li, J. Wang, et al., Appl. Catal. B: Environ. 191 (2016) 94–105.
[38] B. Neppolian, H. Jung, H. Choi, J. Adv. Oxid. Technol. 10 (2007) 369–374.
[39] A.H. Mamaghani, F. Haghighat, C.S. Lee, Chemosphere 219 (2019) 804–825.
[40] M.Z. Guo, C. Poon, Build. Environ. 70 (2013) 102–109.
[41] P. Munafò, G.B. Goffredo, E. Quagliarini, B. Mater., Constr. Build. Mater. 84 (2015) 201–218.
[42] M.Z. Guo, A.M. Ramirez, C.S. Poon, J. Clean. Prod. 112 (2016) 3583–3588.
[43] X.W. Li, W.D. Zhang, J.Y. Li, et al., Appl. Catal. B: Environ. 241 (2019) 187–195.
[44] U. Berardi, R.H. Nosrati, Energy 147 (2018) 1188–1202.
[45] M.Z. Guo, T.C. Ling, C.S. Poon, Environ. Pollut. 273 (2021) 116510–116519.
[46] Z. Liu, Q. Guan, H. Luo, et al., Atmos. Environ. 213 (2019) 515–525.
[47] H.T. Nguyen, K.H. Kim, C. Park, Atmos. Environ. 106 (2015) 347–357.
[48] X. Lyu, H. Guo, I.J. Simpson, et al., Atmos. Chem. Phys. 16 (2016) 6609–6626.
[49] D. Yao, X. Lyu, F. Murray, et al., Sci. Total Environ. 648 (2019) 830–838.
[50] WHO, (2018). https://www.who.int/europe/tools-and-toolkits/airq---software-tool-for-health-risk-assessment-of-air-pollution.